

# Federated Learning over Wireless Networks: Convergence Analysis and Resource Allocation

Canh Dinh, Nguyen H. Tran, Minh N. H. Nguyen, Choong Seon Hong, Wei Bao, Albert Zomaya, Vincent Gramoli

**Abstract**—There is an increasing interest in a fast-growing machine learning technique called Federated Learning, in which the model training is distributed over mobile user equipments (UEs), exploiting UEs' local computation and training data. Despite its advantages in data privacy-preserving, Federated Learning (FL) still has challenges in heterogeneity across users' data and UE's characteristics. We first address the heterogeneous data challenge by proposing a FL algorithm that can bypass the independent and identically distributed (i.i.d.) UEs' data assumption for strongly convex and smooth problems. We provide the convergence rate characterizing the trade-off between local computation rounds of UE to update its local model and global communication rounds to update the global model. We then employ the proposed FL algorithm in wireless networks as a resource allocation optimization problem that captures various trade-offs between computation and communication latencies as well as between the Federated Learning time and UE energy consumption. Even though the wireless resource allocation problem of FL is non-convex, we exploit this problem's structure to decompose it into three sub-problems and analyze their closed-form solutions as well as insights to problem design. Finally, we illustrate the theoretical analysis for the new algorithm with Tensorflow experiments and extensive numerical results for the wireless resource allocation sub-problems. The experiment results not only verify the theoretical convergence but also show that our proposed algorithm converges significantly faster than the existing baseline approach.

**Index Terms**—Distributed Machine Learning over Wireless Networks, Federated Learning, Optimization Decomposition.

## I. INTRODUCTION

The significant increase in the number of cutting-edge mobiles and Internet of Things (IoT) devices results in the phenomenal growth of the data volume generated at the edge network. It has been predicted that in 2025 there will be 80 billion devices connected to the Internet and the global data will achieve 180 trillion gigabytes [2]. However, most of this data is privacy-sensitive in nature. It is not only risky to store this data in data centers but also costly in terms of communication. For example, location-based services such as the app Waze [3], can help users avoid heavy-traffic roads and thus reduce the congestion. However, in this application, users

have to share their own locations to the server and it cannot guarantee that the location of drivers is kept safely. Besides, in order to suggest the optimal route for drivers, Waze collects a large number of data included every road driven to transfer to the data center. Transferring this amount of data requires a high expense in communication and drivers' devices to be connected to the Internet continuously.

In order to maintain the privacy of consumer data [4] and reduce the communication cost, it is necessary to have an emergence of a new class of machine learning techniques that shifts the computation to the edge network where the privacy of data is maintained. One such popular technique is called Federated Learning (FL) [5]. This learning technology allows users to collaboratively build a shared learning model while preserving all training data on their user equipment (UE). In particular, a UE computes the updates to the current global model on its local training data, which is then aggregated and fed-back by a central server, so that all UEs have access to the same global model to compute their new updates. This process is repeated until an accuracy level of the learning model is reached. In this way, the user data privacy is well protected because local training data are not shared, thus differ FL from conventional approaches in data acquisition, storage, and training.

There are several reasons why FL is attracting plenty of interests. Firstly, the modern smart UEs are now able to handle heavy computing tasks of intelligent applications as they are armed with high-performance central-processing units (CPUs), graphics processing units (GPUs), and also integrated AI chip called neural processing unit (e.g., Snapdragon 845, Kirin 980 CPU and Apple A12 Bionic CPU [6]). Being equipped with the latest computing resources at the edge, the model training can be updated locally leading to the reduction in the time to upload raw data to the datacenter. Secondly, the increase in storage capacity, as well as the plethora of sensors (e.g., cameras, microphones, GPS) in UEs enables them to collect a wealth amount of data and store this data locally. This greatly facilitates an unprecedented large-scale flexible data collection and model training. Therefore, with the recent advances in edge computing, FL can be easily implemented in reality. For example, a crowd of smart devices can proactively sense and collect data during the day hours, then they jointly feedback and update the global model during the night hours, to improve the efficiency and accuracy for next-day usage. We envision that such this approach will boost a new generation of smart

C. Dinh, N. H. Tran, W. Bao, A. Zomaya, and V. Gramoli, are with the School of Computer Science, The University of Sydney, Sydney, NSW 2006, Australia (email: tdin6081@uni.sydney.edu.au, {nguyen.tran, wei.bao, albert.zomaya, vincent.gramoli}@sydney.edu.au).

M. N.H. Nguyen and C.S Hong are with the Department of Computer Science and Engineering, Kyung Hee University, Korea (email: {minhnhn, cshong}@khu.ac.kr).

A preliminary version of this paper was presented at IEEE INFOCOM 2019 [1].

services, such as smart transportation, smart shopping, and smart hospital.

With all the promising benefits, FL also comes with new challenges to tackle. On one hand, the numbers of UEs in FL can be large and the data generated at heterogeneous UEs have diverse distributions [5]. Therefore, the training data generated at UEs basically is heterogeneous and non-i.i.d. How to design efficient algorithms to handle statistical heterogeneity with convergence guarantee is thus a priority question. Recently, several studies [5], [7], [8] have used de facto optimization algorithms such as Gradient Descent (GD), Stochastic Gradient Descent (SGD) to enable devices' local updates in FL. One of the most well-known methods [5] named FedAvg using average SGD updates was experimentally shown to perform well in non-i.i.d. UE data settings. However, this work lacks theoretical convergence analysis. By leveraging edge computing to enable FL, [8] proposed algorithms for heterogeneous FL networks by using GD with bounded gradient divergence assumption to facilitate the convergence analysis. In another direction, the idea of allowing UEs to solve the local problems in FL with arbitrary optimization algorithm to obtain a local accuracy (or inexactness level) has attracted a number of researchers [9], [10]. While [9] uses primal-dual analysis to prove the algorithm convergence under any distribution of data, the authors of [10] proposed adding proximal terms to local functions and used primal analysis for convergence proof with a local dissimilarity assumption, a similar idea of bounding the gradient divergence between local and global loss functions. Since the local accuracy level provides an elegant trade-off between local computations and global communication rounds, we aim to design an FL algorithm that can relate an arbitrary local accuracy level to the number of computation rounds, with direct primal convergence analysis, and no assumption on bounding gradient divergence.

While all of the above FL algorithms' complexities are measured in terms of the number of local and global update rounds (or iterations), the wall clock time of FL when deployed in a wireless environment will largely depends on the number of UEs and their diverse characteristics since UEs may have different hardware, energy budget, and wireless connection status. Specifically, the total wall-clock training time of FL includes not only the UE computation time (which depend on UEs' CPU types and local data sizes) but also the communication time of all UEs (which depends on UE channel gains, energy budget, and data size). Thus, to minimize the wall-clock training time of FL, a careful resource allocation problem for FL over wireless networks needs to consider not only the FL parameters such as accuracy level for computation-communication trade-off, but also allocating the UEs' resources such as power and CPU cycles with respect to wireless channels.

For the above two motivations, our contributions are summarized as follows:

- We propose a new FL algorithm with only assumption on strongly convex and smooth problems, named FEDL. The crux of FEDL is a new local surrogate function design

for UEs allowing each UE to solve its local problem approximately, characterized by a hyper-learning rate  $\eta$  and local accuracy level  $\theta$ , respectively. Using primal convergence analysis with the assumption that all UEs use GD to solve their local problems, we show that FEDL can attain a linear convergence rate by controlling  $\eta$  and  $\theta$ , which also provides the trade-off between the number of local computation and global communication rounds. We then employ FEDL on Tensorflow to verify the theoretical findings with several federated datasets. The experimental results show that FEDL outperformed FedAvg in terms of convergence speed.

- We pose a resource allocation problem for FEDL over wireless networks to capture the trade-off between the wall clock training time of FEDL and UE energy consumption by using Pareto efficiency model. To handle the non-convexity of this problem, we exploit its special structure to decompose it into three sub-problems. The first two sub-problems relate to UE resource allocation over wireless networks, which are transformed to be convex and solved separately; then their solutions are used to obtain the solution to the third sub-problem, which is the optimal  $\eta$  and  $\theta$  of FEDL. We derive their closed-form solutions, and characterize the impact of the Pareto-efficient controlling knob to the optimal: (i) computation and communication training time, (ii) UE resource allocation, and (iii) local accuracy level. We also provide extensive numerical results to examine the impact of UE heterogeneity and Pareto curve between UE energy cost and wall clock training time.

The rest of this paper is organized as follows. Section II discusses several works on the FL algorithm and resource allocation. Section III defines our Federated model which contains the learning problem. Section IV shows our algorithm design and analysis. Section V consists of FL over wireless network problems. Experimental performance of FEDL and numerical results of the resource allocation for FEDL over wireless networks are provided in Section VI and Section VII, respectively. Section VIII concludes our work.

## II. RELATED WORKS

Due to Big Data applications and complex models such as Deep Learning, training machine learning models needs to be distributed over multiple machines, giving rise to researches on decentralized machine learning [11]–[16]. However, most of the algorithms in these works are designed for machines having balanced and/or i.i.d. data. Realizing the lack of studies in dealing with unbalanced and non-i.i.d. data, there is an increasing number of researchers who have interests in studying FL, a state-of-the-art distributed machine learning technique [5], [8], [10], [17], [18]. This technique takes advantage of the involvement of a large number of devices where data are self-generated locally that makes them statistically heterogeneous in nature. As a result, designing algorithms with the global model's convergence guaranteed becomes challenging. There are two main approaches to overcome this problem.

The first one is based on de facto algorithm SGD with a fixed number of local iterations on each device [5]. Despite its feasibility, these studies still have limitations as lacking the convergence analysis. The work in [8] takes this approach to the next step by using additional assumptions on Lipschitz local functions and bounded gradient divergence to prove the convergence of the algorithm.

Another useful approach to tackle the heterogeneity challenge is to allow UEs to solve their primal problems approximately up to a local accuracy threshold [10], [13]. Their works show the main benefit of this approximation approach is that it allows flexibility in the compromise between the number of rounds run on the local model update and the communication to the server for the global model update. However, those approaches increase the computation load at local devices by adding proximal parameter control. In terms of distributed setting, several works [13], [19] utilize approximate Newton method by adding averaging computations at each local iteration update to reduce the number of rounds in communication. Although their algorithms show faster convergence time than the gradient descent method, there is still limited research on applying this method on FL. Therefore, our work firstly narrows this gap by proposing a new algorithm for FL which takes advance of [13] with convergence guarantee and solves local problem approximately without additional parameters.

From a different perspective, many researchers have started to pay attention to the efficient wireless communication between UEs and server centers in FL-supported networks [1], [8], [20]–[22]. The work [8] proposed algorithms for FL in the context of edge networks for a typical edge computing architecture but most of their works focused on designing algorithms to improve the convergence of training time. While there are several works [23], [24] take a keen on minimizing communicated messages for each global iteration update by applying sparsification, quantization, it is still a challenge to utilize them in federated environments. For example, [20] uses the gradient quantization, gradient sparsification, and error accumulation to compress gradient message under the wireless multiple-access channel with the assumption of noiseless communication. Similar work has been seen in [21] using the same quantization technique to explore convergence guarantee with low-precision training. Having the idea in figuring out the impacts of wireless resource on minimizing the training time, [22] focused on using cell-free massive MIMO to support FL. However, most of them use standard existing FL algorithms, while we propose a new one. Furthermore, we also study how the computation and communication characteristics of UEs can affect their energy consumption, training time convergence, and an accuracy level of FL considering *heterogeneous* UEs in terms of data size, channel gain, computing, and transmission power capabilities.

### III. SYSTEM MODEL

We consider a wireless multi-user system consisting of one edge server and a set  $\mathcal{N}$  of  $N$  UEs. Each participating UE  $n$  stores a local data set  $\mathcal{D}_n$ , with its size is denoted by  $D_n$ .

Then, we can define the total data size by  $D = \sum_{n=1}^N D_n$ . In an example of the supervised learning setting, at UE  $n$ ,  $\mathcal{D}_n$  defines the collection of data samples given as a set of input-output pairs  $\{x_i, y_i\}_{i=1}^{D_n}$ , where  $x_i \in \mathbb{R}^d$  is an input sample vector with  $d$  features, and  $y_i \in \mathbb{R}$  is the labeled output value for the sample  $x_i$ . The data can be generated through the usage of UE, for example, via interactions with mobile apps.

In a typical learning problem, for a sample data  $\{x_i, y_i\}$  with input  $x_i$  (e.g., the response time of various apps inside the UE), the task is to find the *model parameter*  $w \in \mathbb{R}^d$  that characterizes the output  $y_i$  (e.g., label of edge server load, such as high or low, in next hours) with the loss function  $f_i(w)$ . The loss function on the data set of UE  $n$  is defined as

$$F_n(w) := \frac{1}{D_n} \sum_{i \in \mathcal{D}_n} f_i(w).$$

Then, the learning model is the minimizer of the following global loss function minimization problem

$$\min_{w \in \mathbb{R}^d} F(w) := \sum_{n=1}^N \frac{D_n}{D} F_n(w). \quad (1)$$

**Assumption 1.**  $F_n(\cdot)$  is  $L$ -smooth and  $\beta$ -strongly convex,  $\forall n$ , respectively, as follows,  $\forall w, w' \in \mathbb{R}^d$ :

$$\begin{aligned} F_n(w) &\leq F_n(w') + \langle \nabla F_n(w'), w - w' \rangle + \frac{L}{2} \|w - w'\|^2 \\ F_n(w) &\geq F_n(w') + \langle \nabla F_n(w'), w - w' \rangle + \frac{\beta}{2} \|w - w'\|^2. \end{aligned}$$

Throughout this paper,  $\langle w, w' \rangle$  is inner product of vectors  $w$  and  $w'$ . All of the norms are Euclidean norm. We note that strong convexity and smoothness in Assumption 1, also used in [8], can be found in a wide range of applications such as  $l_2$ -regularized linear regression model with  $f_i(w) = \frac{1}{2}(\langle x_i, w \rangle - y_i)^2 + \frac{\beta}{2} \|w\|^2$ ,  $y_i \in \mathbb{R}$ , and  $l_2$ -regularized logistic regression with  $f_i(w) = \log(1 + \exp(-y_i \langle x_i, w \rangle)) + \frac{\beta}{2} \|w\|^2$ ,  $y_i \in \{-1, 1\}$ .

### IV. FEDERATED LEARNING ALGORITHM DESIGN

In this section, we propose a general FL framework for a distributed machine learning system, named FEDL, as presented in Algorithm 1. We briefly summarize the above algorithm in what follows. To solve problem (1), FEDL uses an iterative approach that requires  $K_g$  *global rounds* for global model updates. In each global round, there are interactions between the UEs and edge server. Specifically, a participating UE, in each computation phase, will update its local model using local training data  $\mathcal{D}_n$  as follows.

**UEs update local models:** In order to obtain the local model  $w_n^t$  at a global round  $t$ , each UE  $n$  will minimize its following surrogate function (line 3)

$$\min_{w \in \mathbb{R}^d} J_n^t(w) := D_{F_n}(w, w^{t-1}) + \eta \hat{F}(w|w^{t-1}), \quad (2)$$

where

$$\begin{aligned} D_{F_n}(w, w^{t-1}) \\ := F_n(w) - F_n(w^{t-1}) - \langle \nabla F_n(w^{t-1}), w - w^{t-1} \rangle \end{aligned}$$

is the Bregman divergence [25] of  $F_n(\cdot)$ ;

$$\hat{F}(w|w^{t-1}) := F(w^{t-1}) + \langle \nabla F(w^{t-1}), w - w^{t-1} \rangle$$

is the first-order approximation of the global function  $F(\cdot)$  at  $w^{t-1}$ , and  $\eta > 0$  is a parameter balancing (or regularizing) the weight between the local and approximated global objectives,  $D_{F_n}(w, w^{t-1})$  and  $\hat{F}(w|w^{t-1})$ , respectively. While the meaning of  $\hat{F}(w|w^{t-1})$  is obvious, Bregman divergence, which is a convex function, can be seen as the distance between two points that can generalize the square Euclidean distance and have a lot of applications in machine learning, statistics, and information geometry [25]. Indeed, from strong convexity property in Assumption 1, we have  $D_{F_n}(w, w^{t-1}) \geq \frac{\beta}{2} \|w - w^{t-1}\|^2$ . Thus minimizing  $D_{F_n}(w, w^{t-1})$  implies minimizing not only  $F_n(\cdot)$  but also the distance between  $w$  and  $w^{t-1}$ , which helps stabilize the local update not far away from the ‘‘anchor point’’  $w^{t-1}$ . By removing all constant terms, we can succinctly rewrite  $J_n^t(\cdot)$  as follows

$$J_n^t(w) = F_n(w) + \langle \eta \nabla F(w^{t-1}) - \nabla F_n(w^{t-1}), w \rangle. \quad (3)$$

One of the key ideas of FEDL is UEs can solve (3) approximately to obtain an approximation solution  $w_n^t$  satisfying

$$\|\nabla J_n(w_n^t)\| \leq \theta \|\nabla J_n(w^{t-1})\|, \forall n, \quad (4)$$

which is parametrized by a local accuracy  $\theta \in (0, 1)$  that is common to all UEs. This local accuracy concept resembles the approximate factors in [9], [19]. Here  $\theta = 0$  means the local problem (2) is required to be solved optimally, and  $\theta = 1$  means no progress for local problem, e.g., by setting  $w_n^t = w^{t-1}$ . The surrogate function  $J_n^t$  is motivated from the scheme Distributed Approximate Newton (DANE) proposed in [13]. However, DANE requires (i) additional proximal terms (i.e.,  $\frac{\mu}{2} \|w - w^{t-1}\|^2$ ) and assumption that UEs’ samples are i.i.d. (i.e., not true for FL context) so that the Hessians  $\nabla^2 F_n(w)$  are similar to each other, on which their convergence proof relied, and (ii) solving local problem (2) exactly (i.e.,  $\theta = 0$ ), whereas FEDL, without proximal terms, avoids an additional controlling parameter (i.e.,  $\mu$ ), and flexibly solves local problem approximately by controlling  $\theta$ .

Assuming that UEs use an available de-facto optimization algorithm for machine learning (e.g., gradient descent), then minimizing the local problem (2) to achieve the accuracy threshold  $\theta$  also takes  $K_l$  local rounds, which depends on  $\theta$  (to be shown later in Lemma 1).

**Edge server updates global model:** The edge server then aggregates the local model  $w_n^t$  to update the following parameters

$$w^t = \sum_{n=1}^N \frac{D_n}{D} w_n^t, \quad (5)$$

and then broadcast  $w^t$  and  $\nabla F(w^t)$  to all UEs (line 5), which are required for participating UEs to minimize their surrogate  $J_n^{t+1}$  in the next global round  $t+1$ . We see that the edge server does not access the local data  $D_n$ ,  $\forall n$ , thus preserving data

---

#### Algorithm 1 FEDL

---

- 1: **Input:**  $w^0$ ,  $\theta \in [0, 1]$ ,  $\epsilon$ .
  - 2: **for**  $t = 1$  to  $K_g$  **do**
  - 3:   **Computation:** Each UE  $n$  solves its local problem (2) in  $K_l$  rounds to achieve  $\theta$ -approximate  $w_n^t$  satisfying (4).
  - 4:   **Communication:** All UEs transmit  $w_n^t$  to the edge server.
  - 5:   **Aggregation and Feedbacks:** The edge server updates the global model as in (5) and then fed-backs  $w^t$  and  $\nabla F(w^t)$  to all UEs.
- 

privacy. For an arbitrary small constant  $\epsilon > 0$ , the problem (1) achieves a global model convergence  $w^t$  when it satisfies

$$F(w^t) - F(w^*) \leq \epsilon, \forall t \geq K_g, \quad (6)$$

where  $w^*$  is the optimal solution to (1).

Next, we will provide the convergence analysis for FEDL. We see that  $J_n^t(w)$  is also  $\beta$ -strongly convex and  $L$ -smooth as  $F_n(\cdot)$  because they have the same Hessian matrix. With these properties of  $J_n^t(w)$ , we can use GD<sup>1</sup> to solve (2) as follows

$$z^{k+1} = z^k - h_k \nabla J_n^t(z^k), \quad (7)$$

where  $h_k$  is a predefined learning rate, which has been shown to generate a convergent sequence  $(z_k)_{k \geq 0}$  satisfying a linear convergence rate [26] as follows

$$J_n^t(z_k) - J_n^t(z^*) \leq c(1 - \gamma)^k (J_n^t(z_0) - J_n^t(z^*)), \quad (8)$$

where  $z^*$  is the optimal solution to the local problem (2), and  $c$  and  $\gamma \in (0, 1)$  are constants depending on  $L$  and  $\beta$ .

**Lemma 1.** *With Assumption 1 and the assumed linear convergence rate (8) with  $z_0 = w^{t-1}$ , the number of local rounds for solving (2) to achieve a  $\theta$ -approximation condition (4) is*

$$K_l = \frac{2}{\gamma} \log \frac{C}{\theta}, \quad (9)$$

where  $C := c \frac{L}{\beta}$ .

**Theorem 1.** *With Assumption 1, the convergence of FEDL is achieved with linear rate*

$$F(w^t) - F(w^*) \leq (1 - \Theta)^k (F(w^{(0)}) - F(w^*)), \quad (10)$$

where  $\Theta \in (0, 1)$  is defined as

$$\Theta := \frac{2\eta L}{\beta} \left[ (1 - \theta)^2 \frac{\beta^2}{L^2} - \theta(1 + \theta) - (1 + \theta)^2 \frac{\eta}{2} \right]. \quad (11)$$

**Corollary 1.** *The number of global rounds for FEDL to achieve the convergence satisfying (6) is*

$$K_g = \frac{1}{\Theta} \log \frac{\Delta_g}{\epsilon}, \quad (12)$$

<sup>1</sup>GD method is reasonable when each UE holds a small portion of samples, i.e.,  $D_n \ll D$ ,  $\forall n$ . In case of large  $D_n$ , SGD with mini-batch can be used to alleviate the computation burden on UEs, but the analysis will be different. In Section VI, we show experiment performance of FEDL using both GD and mini-batch SGD.

where  $\Delta_g := F(w^0) - F(w^*)$ .

The proof of this corollary can be shown similarly to that of Lemma 1. We have some following remarks:

- 1) The convergence of FEDL can always be obtained by setting sufficiently small values of both  $\eta$  and  $\theta \in (0, 1)$  such that  $\Theta \in (0, 1)$ . To see that, the inside-bracket terms on the right hand side of (11) can be rewritten as  $A - B$ , where  $A = (1 - \theta)^2 \frac{\beta^2}{L^2} - \theta(1 + \theta)$  and  $B = (1 + \theta)^2 \frac{\eta}{2}$ . Since  $\lim_{\theta \rightarrow 0} A = \frac{\beta^2}{L^2}$  and  $\lim_{\eta \rightarrow 0} B = 0$ , there exists small values of  $\theta$  and  $\eta$  such that  $A - B > 0$ , thus  $\Theta > 0$ . On the other hand, we have  $\lim_{\eta \rightarrow 0} \Theta = 0$ ; thus, there exists a small value of  $\eta$  such that  $\Theta < 1$ .
- 2) There is a convergence trade-off between the number of local and global rounds characterized by  $\theta$ : small  $\theta$  makes large  $K_l$ , but small  $K_g$ , according to (9) and (12), respectively. This trade-off was also observed by authors of [9], though their technique (i.e., primal-dual optimization) is different from ours. This trade-off is intuitive: if UEs focus on solving their local problems more exactly, then FEDL requires fewer number of communication exchanges between the edge server and UEs, and vice versa.
- 3) While  $\theta$  affects to both local and global convergence,  $\eta$  only affects to the global convergence rate of FEDL. If  $\eta$  is too small, so is  $\Theta$ , which makes FEDL have more global rounds with large  $K_g$ . However, if  $\eta$  is large enough,  $\Theta$  may not be in  $(0, 1)$ , which leads to the divergence of FEDL. With these properties similar to the learning rate  $h_k$  in (7) for the local problem (2), we can consider  $\eta$  as the *hyper-learning rate* for the global problem (1).

The time complexity of FEDL in this section is represented by  $K_g$  global rounds (i.e., communication rounds) and  $K_l$  local rounds (i.e., computation rounds). Even though FEDL convergence is independent of the number of UEs (c.f. (12)), when implementing FEDL over wireless networks, the wall clock time of each communication round can be significantly larger than that of computation if the number of UEs increases, due to multi-user contention for wireless medium. In the next section, we will study the UE resource allocation to enable FEDL over wireless networks.

## V. FEDL OVER WIRELESS NETWORKS

In this section, we first present the system model and problem formulation of the UE resource allocation supporting FEDL over a time-sharing wireless environment. We then decompose this problem into three sub-problems, derive their closed-form solutions, reveal the hindsights, and provide numerical support.

### A. System Model

At first, we consider synchronous communication which requires all UEs to finish solving their local problems before entering the communication phase. During the communication phase, the model's updates are transferred to the edge server

by using a wireless medium sharing scheme. In the communication phase, each global round consists of computation and communication time which includes uplink and downlink ones. In this work, however, we do not consider the downlink communication time as it is negligible compared to the uplink one. The reason is that the downlink has larger bandwidth than the uplink and the edge server power is much higher than UE's transmission power. Besides, the computation time only depends on the number of local rounds, and thus  $\theta$ , according to (9). Denoting the time of one local round by  $T_{cp}$ , i.e., the time to computing one local round (8), then the computation time in one global round is  $K_l T_{cp}$ . Denoting the communication time in one global round by  $T_{co}$ , the wall clock time of one global round of FEDL is defined as

$$T_g := T_{co} + K_l T_{cp}.$$

1) *Computation Model*: We denote the number of CPU cycles for UE  $n$  to execute one sample of data by  $c_n$ , which can be measured offline [27] and is known a priori. Since all samples  $\{x_i, y_i\}_{i \in \mathcal{D}_n}$  have the same size (i.e., number of bits), the number of CPU cycles required for UE  $n$  to run one local round is  $c_n D_n$ . Denote the CPU-cycle frequency of the UE  $n$  by  $f_n$ . Then the CPU energy consumption of UE  $n$  for one local round of computation can be expressed as follows [28]

$$E_{n,cp} = \sum_{i=1}^{c_n D_n} \frac{\alpha_n}{2} f_n^2 = \frac{\alpha_n}{2} c_n D_n f_n^2, \quad (13)$$

where  $\alpha_n/2$  is the effective capacitance coefficient of UE  $n$ 's computing chipset. Furthermore, the computation time per local round of the UE  $n$  is  $\frac{c_n D_n}{f_n}$ ,  $\forall n$ . We denote the vector of  $f_n$  by  $f \in \mathbb{R}^n$ .

2) *Communication Model*: In FEDL, regarding to the communication phase of UEs, we consider a time-sharing multi-access protocol (similar to TDMA) for UEs. We note that this time-sharing model is not restrictive because other schemes, such as OFDMA, can also be applied to FEDL. The achievable transmission rate (nats/s) of UE  $n$  is defined as follows:

$$r_n = B \ln\left(1 + \frac{h_n p_n}{N_0}\right), \quad (14)$$

where  $B$  is the bandwidth,  $N_0$  is the background noise,  $p_n$  is the transmission power, and  $h_n$  is the channel gain of the UE  $n$ . We assume that  $h_n$  is constant during the training time of FEDL<sup>2</sup>. Denote the fraction of communication time allocated to UE  $n$  by  $\tau_n$ , and the data size (in nats) of  $w_n$  by  $s_n$ . Because the dimension of vector  $w_n$  are fixed, we assume that their sizes are constant throughout the FEDL learning. Then the transmission rate of each UE  $n$  is

$$r_n = s_n / \tau_n, \quad (15)$$

which is shown to be the most energy-efficient transmission policy [29]. Thus, to transmit  $s_n$  within a time duration  $\tau_n$ , the UE  $n$ 's energy consumption is

$$E_{n,co} = \tau_n p_n (s_n / \tau_n), \quad (16)$$

<sup>2</sup>For the case of stochastic  $h_n$ , refer to the model in [22].

where the power function is

$$p_n(s_n/\tau_n) := \frac{N_0}{h_n} \left( e^{\frac{s_n/\tau_n}{B}} - 1 \right) \quad (17)$$

according to (14) and (15). We denote the vector of  $\tau_n$  by  $\tau \in \mathbb{R}^n$ .

Define the total energy consumption of all UEs for each global round by  $E_g$ , which is expressed as follows:

$$E_g := \sum_{n=1}^N E_{n,co} + K_l E_{n,cp}.$$

### B. Problem formulation

We consider an optimization problem, abusing the same name FEDL, as follows

$$\begin{aligned} & \underset{f, \tau, \theta, \eta, T_{co}, T_{cp}}{\text{minimize}} && K_g(E_g + \kappa T_g) \\ & \text{subject to} && \sum_{n=1}^N \tau_n \leq T_{co}, \end{aligned} \quad (18)$$

$$\max_n \frac{c_n D_n}{f_n} = T_{cp}, \quad (19)$$

$$f_n^{\min} \leq f_n \leq f_n^{\max}, \quad \forall n \in \mathcal{N}, \quad (20)$$

$$p_n^{\min} \leq p_n(s_n/\tau_n) \leq p_n^{\max}, \quad \forall n \in \mathcal{N}, \quad (21)$$

$$0 \leq \theta \leq 1. \quad (22)$$

Minimize both UEs' energy consumption and the FL time are conflicting. For example, the UEs can save the energy by setting the lowest frequency level all the time, but this will certainly increase the training time. Therefore, to strike the balance between energy cost and training time, the weight  $\kappa$  (Joules/second), used in the objective as an amount of additional energy cost that FEDL is willing to bear for one unit of training time to be reduced, captures the Pareto-optimal tradeoff between the UEs' energy cost and the FL time. For example, when most of the UEs are plugged in, then UE energy is not the main concern, thus  $\kappa$  can be large. According to optimization theory,  $1/\kappa$  also plays the role of a Lagrange multiplier for a "hard constraint" on UE energy [30].

While constraint (18) captures the time-sharing uplink transmission of UEs, constraint (19) defines that the computing time in one local round is determined by the "bottleneck" UE (e.g., with large data size and low CPU frequency). The feasible regions of CPU-frequency and transmit power of UEs are imposed by constraints (20) and (21), respectively. We note that (20) and (21) also capture the heterogeneity of UEs with different types of CPU and transmit chipsets. The last constraint restricts the feasible range of the local accuracy.

### C. Solutions to FEDL

We see that FEDL is non-convex due to the constraint (19) and several products of two functions in the objective function. However, in this section we will characterize FEDL's optimal solution by decomposing it into multiple convex sub-problems.

We consider the first case when  $\theta$  and  $\eta$  are fixed, then FEDL can be decomposed into two sub-problems as follows:

$$\begin{aligned} \text{SUB1:} \quad & \underset{f, T_{cp}}{\text{minimize}} && \sum_{n=1}^N E_{n,cp} + \kappa T_{cp} \\ & \text{subject to} && \frac{c_n D_n}{f_n} \leq T_{cp}, \quad \forall n \in \mathcal{N}, \\ & && f_n^{\min} \leq f_n \leq f_n^{\max}, \quad \forall n \in \mathcal{N}. \end{aligned} \quad (23)$$

$$\begin{aligned} \text{SUB2:} \quad & \underset{\tau, T_{co}}{\text{min.}} && \sum_{n=1}^N E_{n,co} + \kappa T_{co} \\ & \text{s.t.} && \sum_{n=1}^N \tau_n \leq T_{co}, \\ & && p_n^{\min} \leq p_n(s_n/\tau_n) \leq p_n^{\max}, \quad \forall n. \end{aligned} \quad (24)$$

While SUB1 is a CPU-cycle control problem for the computation time and energy minimization, SUB2 can be considered as an uplink power control to determine the UEs' fraction of time sharing to minimize the UEs' energy and communication time. We note that the constraint (19) of FEDL is replaced by an equivalent one (23) in SUB1. We can consider  $T_{cp}$  and  $T_{co}$  as virtual deadlines for UEs to perform their computation and communication updates, respectively. It can be observed that both SUB1 and SUB2 are convex problems.

1) *SUB1 Solution:* We first propose Algorithm 2 in order to categorize UEs into one of three groups:  $\mathcal{N}_1$  is a group of "bottleneck" UEs that always run its maximum frequency;  $\mathcal{N}_2$  is the group of "strong" UEs which can finish their tasks before the computational virtual deadline even with the minimum frequency; and  $\mathcal{N}_3$  is the group of UEs having the optimal frequency inside the interior of their feasible sets.

**Lemma 2.** *The optimal solution to SUB1 is as follows*

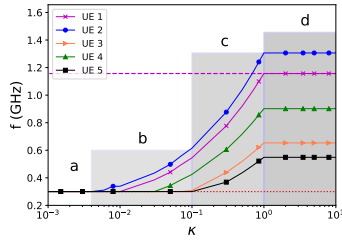
$$f_n^* = \begin{cases} f_n^{\max}, & \forall n \in \mathcal{N}_1, \\ f_n^{\min}, & \forall n \in \mathcal{N}_2, \\ \frac{c_n D_n}{T_{cp}^*}, & \forall n \in \mathcal{N}_3, \end{cases} \quad (26)$$

$$T_{cp}^* = \max\{T_{\mathcal{N}_1}, T_{\mathcal{N}_2}, T_{\mathcal{N}_3}\}, \quad (27)$$

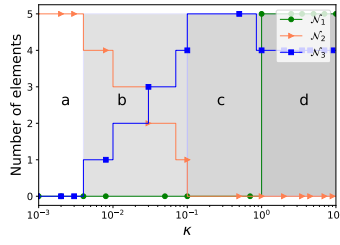
where  $\mathcal{N}_1, \mathcal{N}_2, \mathcal{N}_3 \subseteq \mathcal{N}$  are three subsets of UEs produced by Algorithm 2 and

$$\begin{aligned} T_{\mathcal{N}_1} &= \max_{n \in \mathcal{N}} \frac{c_n D_n}{f_n^{\max}}, \\ T_{\mathcal{N}_2} &= \max_{n \in \mathcal{N}_2} \frac{c_n D_n}{f_n^{\min}}, \\ T_{\mathcal{N}_3} &= \left( \frac{\sum_{n \in \mathcal{N}_3} \alpha_n (c_n D_n)^3}{\kappa} \right)^{1/3}. \end{aligned} \quad (28)$$

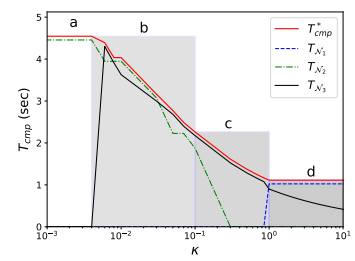
From Lemma 2, first, we see that the optimal solution depends not only on the existence of these subsets, but also on their virtual deadlines  $T_{\mathcal{N}_1}$ ,  $T_{\mathcal{N}_2}$ , and  $T_{\mathcal{N}_3}$ , in which the longest of them will determine the optimal virtual deadline  $T_{cp}^*$ . Second, from (26), the optimal frequency of each UE will depend on both  $T_{cp}^*$  and the subset it belongs to. We note that depending on  $\kappa$ , some of the three sets (not all) are possibly empty sets, and by default  $T_{\mathcal{N}_i} = 0$  if  $\mathcal{N}_i$  is an empty



(a) Optimal CPU frequency of each UE.



(b) Three subsets outputted by Alg. 2.



(c) Optimal computation time.

Fig. 1: Solution to SUB1 with five UEs. For wireless communication model, the UE channel gains follow the exponential distribution with the mean  $g_0(d_0/d)^4$  where  $g_0 = -40$  dB and the reference distance  $d_0 = 1$  m. The distance between these devices and the wireless access point is uniformly distributed between 2 and 50 m. In addition,  $B = 1$  MHz,  $\sigma = 10^{-10}$  W, the transmission power of devices are limited from 0.2 to 1 W. For UE computation model, we set the training size  $D_n$  of each UE as uniform distribution in 5 – 10 MB,  $c_n$  is uniformly distributed in 10 – 30 cycles/bit,  $f_n^{max}$  is uniformly distributed in 1.0 – 2.0 GHz,  $f_n^{min} = 0.3$  GHz. Furthermore,  $\alpha = 2 \times 10^{-28}$  and the UE update size  $s_n = 25,000$  nats ( $\approx 4.5$  KB).

### Algorithm 2 Finding $\mathcal{N}_1, \mathcal{N}_2, \mathcal{N}_3$ in Lemma 2

- 1: Sort UEs such that  $\frac{c_1 D_1}{f_n^{min}} \leq \frac{c_2 D_2}{f_n^{min}} \leq \dots \leq \frac{c_N D_N}{f_n^{min}}$
- 2: **Input:**  $\mathcal{N}_1 = \emptyset, \mathcal{N}_2 = \emptyset, \mathcal{N}_3 = \mathcal{N}, T_{N_3}$  in (28)
- 3: **for**  $i = 1$  to  $N$  **do**
- 4:   **if**  $\max_{n \in \mathcal{N}} \frac{c_n D_n}{f_n^{max}} \geq T_{N_3} > 0$  and  $\mathcal{N}_1 == \emptyset$  **then**
- 5:      $\mathcal{N}_1 = \mathcal{N}_1 \cup \{m : \frac{c_m D_m}{f_m^{max}} = \max_{n \in \mathcal{N}} \frac{c_n D_n}{f_n^{max}}\}$
- 6:      $\mathcal{N}_3 = \mathcal{N}_3 \setminus \mathcal{N}_1$  and update  $T_{N_3}$  in (28)
- 7:   **if**  $\frac{c_i D_i}{f_i^{min}} \leq T_{N_3}$  **then**
- 8:      $\mathcal{N}_2 = \mathcal{N}_2 \cup \{i\}$
- 9:      $\mathcal{N}_3 = \mathcal{N}_3 \setminus \{i\}$  and update  $T_{N_3}$  in (28)

set,  $i = 1, 2, 3$ . Next, by varying  $\kappa$ , we observe the following special cases.

**Corollary 2.** *The optimal solution to SUB1 can be divided into four regions as follows.*

- a)  $\kappa \leq \min_{n \in \mathcal{N}} \alpha_n (f_n^{min})^3$ :  
 $\mathcal{N}_1$  and  $\mathcal{N}_3$  are empty sets. Thus,  $\mathcal{N}_2 = \mathcal{N}$ ,  $T_{co} = T_{N_2} = \max_{n \in \mathcal{N}} \frac{c_n D_n}{f_n^{min}}$ , and  $f_n^* = f_n^{min}, \forall n \in \mathcal{N}$ .
- b)  $\min_{n \in \mathcal{N}} \alpha_n (f_n^{min})^3 < \kappa \leq (\max_{n \in \mathcal{N}_2} \frac{c_n D_n}{f_n^{min}})^3$ :  
 $\mathcal{N}_2$  and  $\mathcal{N}_3$  are non-empty sets, whereas  $\mathcal{N}_1$  is empty. Thus,  $T_{cp}^* = \max\{T_{N_2}, T_{N_3}\}$ , and  $f_n^* = \max\{\frac{c_n D_n}{T_{cp}^*}, f_n^{min}\}, \forall n \in \mathcal{N}$ .
- c)  $(\max_{n \in \mathcal{N}_2} \frac{c_n D_n}{f_n^{min}})^3 < \kappa \leq \frac{\sum_{n \in \mathcal{N}_3} \alpha_n (c_n D_n)^3}{(\max_{n \in \mathcal{N}} \frac{c_n D_n}{f_n^{max}})^3}$ :  
 $\mathcal{N}_1$  and  $\mathcal{N}_2$  are empty sets. Thus  $\mathcal{N}_3 = \mathcal{N}$ ,  $T_{cp}^* = T_{N_3}$ , and  $f_n^* = \frac{c_n D_n}{T_{N_3}}, \forall n \in \mathcal{N}$ .
- d)  $\kappa > \frac{\sum_{n \in \mathcal{N}_3} \alpha_n (c_n D_n)^3}{(\max_{n \in \mathcal{N}} \frac{c_n D_n}{f_n^{max}})^3}$ :  
 $\mathcal{N}_1$  is non-empty. Thus  $T_{cp}^* = T_{N_1}$ , and

$$f_n^* = \begin{cases} f_n^{max}, & \forall n \in \mathcal{N}_1, \\ \max\{\frac{c_n D_n}{T_{N_1}}, f_n^{min}\}, & \forall n \in \mathcal{N} \setminus \mathcal{N}_1. \end{cases} \quad (29)$$

We illustrate Corollary 2 in Fig. 1 with four regions<sup>3</sup> as follows.

- a) Very low  $\kappa$  (i.e.,  $\kappa \leq 0.004$ ): Designed for solely energy minimization. In this region, all UE runs their CPU at the lowest cycle frequency  $f_n^{min}$ , thus  $T_{cp}^*$  is determined by the last UEs that finish their computation with their minimum frequency.
- b) Low  $\kappa$  (i.e.,  $0.004 \leq \kappa \leq 0.1$ ): Designed for prioritized energy minimization. This region contains UEs of both  $\mathcal{N}_2$  and  $\mathcal{N}_3$ .  $T_{cp}^*$  is governed by which subset has higher virtual computation deadline, which also determines the optimal CPU-cycle frequency of  $\mathcal{N}_3$ . Other UEs with light-loaded data, if exist, can run at the most energy-saving mode  $f_n^{min}$  yet still finish their task before  $T_{cp}^*$  (i.e.,  $\mathcal{N}_2$ ).
- c) Medium  $\kappa$  (i.e.,  $0.1 \leq \kappa \leq 1$ ): Designed for balancing computation time and energy minimization. All UEs belong to  $\mathcal{N}_3$  with their optimal CPU-cycle frequency strictly inside the feasible set.
- d) High  $\kappa$  (i.e.,  $\kappa \geq 1$ ): Designed for prioritized computation time minimization. High value  $\kappa$  can ensure the existence of  $\mathcal{N}_1$ , consisting the most “bottleneck” UEs (i.e., heavy-loaded data and/or low  $f_n^{max}$ ) that runs their maximum CPU-cycle in (29) (top) and thus determines the optimal computation time  $T_{cp}^*$ . The other “non-bottleneck” UEs either (i) adjust a “right” CPU-cycle to save the energy yet still maintain their computing time the same as  $T_{cp}^*$  (i.e.,  $\mathcal{N}_3$ ), or (ii) can finish the computation with minimum frequency before the “bottleneck” UEs (i.e.,  $\mathcal{N}_2$ ) as in (29) (bottom).

2) **SUB2 Solution:** Before characterizing the solution to SUB2, from (17) and (25), we first define two bounded values for  $\tau_n$  as follows

$$\tau_n^{max} = \frac{s_n}{B \ln(h_n N_0^{-1} p_n^{min} + 1)},$$

$$\tau_n^{min} = \frac{s_n}{B \ln(h_n N_0^{-1} p_n^{max} + 1)},$$

<sup>3</sup>All closed-form solutions are also verified by the solver IPOPT [31].

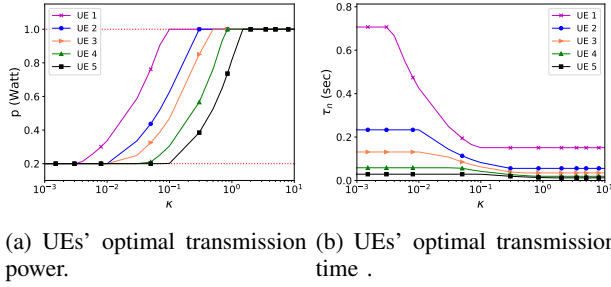


Fig. 2: The solution to SUB2 with five UEs. The numerical setting is the same as that of Fig. 1.

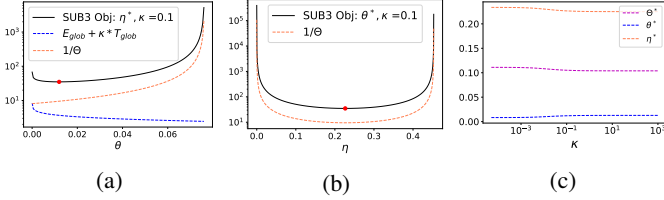


Fig. 3: The solution to SUB3 with five UEs: a) Given  $\eta^*$ , b) Given  $\theta^*$ , and c) Impact of  $\kappa$  on  $\eta^*$ ,  $\theta^*$ , and  $\Theta^*$ . The numerical setting is the same as that of Fig. 1 and the learning parameters is set as  $L = 1, \beta = 0.5, \gamma = 0.5$ , and  $c = 1$ .

which are the maximum and minimum possible fractions of  $T_{co}$  that UE  $n$  can achieve by transmitting with its minimum and maximum power, respectively. We also define a new function  $g_n : \mathbb{R} \rightarrow \mathbb{R}$  as

$$g_n(\kappa) = \frac{s_n/B}{1 + W\left(\frac{\kappa N_0^{-1} h_n - 1}{e}\right)},$$

where  $W(\cdot)$  is the Lambert  $W$ -function. We can consider  $g_n(\cdot)$  as an indirect “power control” function that helps UE  $n$  control the amount of time it should transmit an amount of data  $s_n$  by adjusting the power based on the weight  $\kappa$ . This function is strictly decreasing (thus its inverse function  $g_n^{-1}(\cdot)$  exists) reflecting that when we put more priority on minimizing the communication time (i.e., high  $\kappa$ ), UE  $n$  should raise the power to finish its transmission with less time (i.e., low  $\tau_n$ ).

**Lemma 3.** *The solution to SUB2 is as follows*

a) If  $\kappa \leq g_n^{-1}(\tau_n^{max})$ , then

$$\tau_n^* = \tau_n^{max}$$

b) If  $g_n^{-1}(\tau_n^{max}) < \kappa < g_n^{-1}(\tau_n^{min})$ , then

$$\tau_n^{min} < \tau_n^* = g_n(\kappa) < \tau_n^{max}$$

c) If  $\kappa \geq g_n^{-1}(\tau_n^{min})$ , then

$$\tau_n^* = \tau_n^{min},$$

and  $T_{co}^* = \sum_{n=1}^N \tau_n^*$ .

This lemma can be explained through the lens of network economics. If we interpret the FEDL system as the buyer and UEs as sellers with the UE powers as commodities, then the

inverse function  $g_n^{-1}(\cdot)$  is interpreted as the price of energy that UE  $n$  is willing to accept to provide power service for FEDL to reduce the training time. There are two properties of this function: (i) the price increases with respect to UE power, and (ii) the price sensitivity depends on UEs characteristics, e.g., UEs with better channel quality can have lower price, whereas UEs with larger data size  $s_n$  will have higher price. Thus, each UE  $n$  will compare its energy price  $g_n^{-1}(\cdot)$  with the “offer” price  $\kappa$  by the system to decide how much power it is willing to “sell”. Then, there are three cases corresponding to the solutions to SUB2.

- Low offer: If the offer price  $\kappa$  is lower than the minimum price request  $g_n^{-1}(\tau_n^{max})$ , UE  $n$  will sell its lowest service by transmitting with the minimum power  $p_n^{min}$ .
- Medium offer: If the offer price  $\kappa$  is within the range of an acceptable price range, UE  $n$  will find a power level such that the corresponding energy price will match the offer price.
- High offer: If the offer price  $\kappa$  is higher than the maximum price request  $g_n^{-1}(\tau_n^{min})$ , UE  $n$  will sell its highest service by transmitting with the maximum power  $p_n^{max}$ .

Lemma 3 is further illustrated in Fig. 2, showing how the solution to SUB2 varies with respect to  $\kappa$ . It is observed from this figure that due to the UE heterogeneity of channel gain,  $\kappa = 0.1$  is a medium offer to UEs 2, 3, and 4, but a high offer to UE 1, and low offer to UE 5.

While SUB1 and SUB2 solutions share the same threshold-based dependence, we observe their differences as follows. In SUB1 solution, the optimal CPU-cycle frequency of UE  $n$  depends on the optimal  $T_{cp}^*$ , which in turn depends on the loads (i.e.,  $\frac{c_n D_n}{f_n}, \forall n$ ) of all UEs. Thus all UE load information is required for the computation phase. On the other hand, in SUB2 solution, each UE  $n$  can independently choose its optimal power by comparing its price function  $g_n^{-1}(\cdot)$  with  $\kappa$  so that collecting UE information is not needed. The reason is that the synchronization of computation time in constraint (23) of SUB1 requires all UE loads, whereas the UEs’ time-sharing constraint (24) of SUB2 can be decoupled by comparing with the fixed “offer” price  $\kappa$ .

3) **SUB3 Solution:** We observe that the solutions to SUB1 and SUB2 have no dependence on  $\theta$  so that the optimal  $T_{co}^*$ ,  $T_{cp}^*$ ,  $f^*$ ,  $\tau^*$ , and thus the corresponding optimal energy values, denoted by  $E_{n,cp}^*$  and  $E_{n,cp}^*$ , can be determined based on  $\kappa$  according to Lemmas 2 and 3. However, these solutions will affect to the third sub-problem of FEDL, as will be shown in what follows.

**SUB3:**

$$\begin{aligned} & \underset{\theta, \eta}{\text{minimize}} \quad \frac{1}{\Theta} \left( \sum_{n=1}^N E_{n,co}^* + K_l E_{n,cp}^* + \kappa (T_{co}^* + K_l T_{cp}^*) \right) \\ & \text{subject to} \quad 0 < \Theta < 1, 0 < \theta < 1, \eta > 0. \end{aligned}$$

SUB3 is unfortunate non-convex. However, since there are only two variables to optimize, we can employ numerical methods to find the optimal solution. We plot SUB3 global objective function when fixing  $\eta^*$  or  $\theta^*$  and the impact of

$\kappa$  on learning parameter selection in Fig. 3. Specifically, the global cost regarding UE energy and training time decreases while the number of global iterations will be increased as we reduce the quality of the local problem (i.e., increasing  $\theta$  and hyper-learning rate  $\eta$  is fixed). If we change one of either  $\eta$  or  $\theta$  (and fix the other), the objective function of SUB3 has a convex shape. Besides, the  $\kappa$  parameter also impacts to the learning parameters selection such that the higher  $\kappa$  values lead to higher  $\theta$  and lower  $\eta$  values.

4) *FEDL Solution*: Assuming that we can obtain the optimal solution to SUB3, then we have

**Theorem 2.** *The combined solutions to three sub-problems SUB1, SUB2, and SUB3 are stationary points of FEDL.*

The proof of this theorem is straightforward. The idea is to use the KKT condition to find the stationary points of FEDL. Then we can decompose the KKT condition into three independent groups of equations (i.e., no coupling variables between them), in which the first two groups matches exactly to the KKT conditions of SUB1 and SUB2 that can be solved by closed-form solutions as in Lemmas 2, 3, and the last group for SUB3 is solved by numerical methods.

We then have some discussions on the combined solution to FEDL. First, we see that SUB1 and SUB2 solutions can be characterized independently, which can be explained that each UE often has two separate processors: one CPU for mobile applications and another baseband processor for radio control function. Second, neither SUB1 nor SUB2 depends on  $\theta$  because the communication phase in SUB2 is clearly not affected by the local accuracy of the computing problem, whereas SUB2 considers the computation cost in one local round. However, the solutions to SUB1 and SUB2, which can reveal how much communication cost is more expensive than computation cost, are decisive factors to determine the optimal level of local accuracy. Therefore, we can sequentially solve SUB1 and SUB2 first, then SUB3 to achieve the optimal solutions to FEDL.

## VI. EXPERIMENTS

This section will cover the validation of the FEDL's learning performance in the heterogeneous network. The experiment results not only show the empirical convergence guarantee but also present the significant outperformance of FEDL compared to the FedAvg [5]. All codes and data are published on GitHub [32].

**Experimental settings:** In our setting, the performance of FEDL is examined by image classification tasks using multinomial logistic regression with cross-entropy error loss function (convex models) on different federated datasets (MNIST [33] and FEMNIST [34]). All datasets are split randomly with 75% for training and 25% for testing.

During the experiment, we consider 30 UEs concurrently taking part in the training process. In order to generate datasets capturing the heterogeneous nature of FL, for MNIST dataset, each UE contains only two different labels over the total of 10 labels and each of them has different sample sizes based

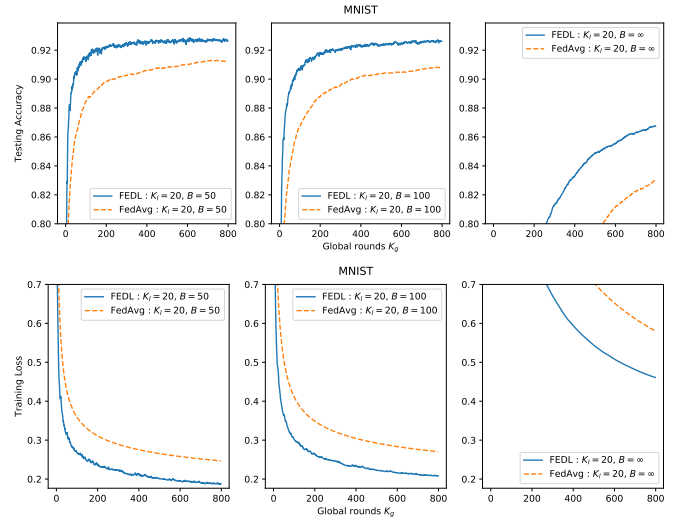


Fig. 4: Effect of different batch size with fixed value of  $K_l$  ( $B = \infty$  means full batch size) on FEDL's performance.

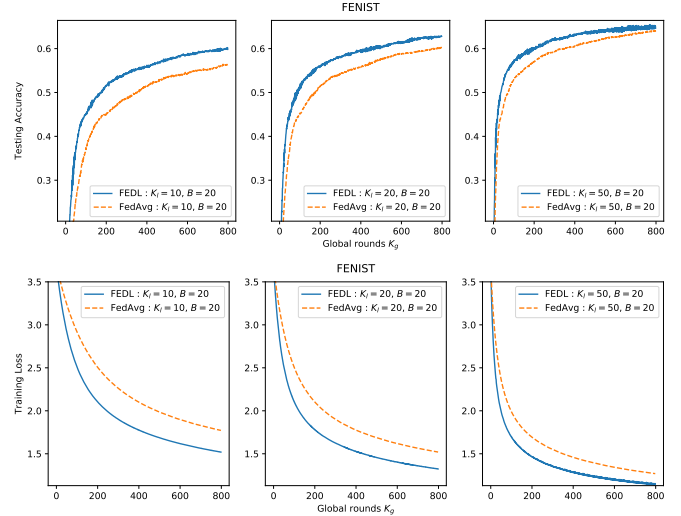


Fig. 5: Effect of increasing local computation time on the convergence of FEDL.

on the power law in [10]; while FEMNIST dataset is built by partitioning the data in Extended MNIST [35] (62 labels) based on the writer of the digit or character and every UE is considered as a writer. The number of data samples for each UE is in the ranges of [15,4492] and [184,334] for MNIST and FEMNIST respectively.

**Effect of different gradient descent algorithms on FEDL's performance:** As UEs are allowed to use different gradient descent methods to minimize the local problem (5), the convergence of FEDL can be evaluated on different optimization algorithms: GD and Mini-Batch SGD by changing the configuration of the batch size during the local training process. While a full batch size is applied for GD, Mini-Batch SGD is trained with a batch size of 50 and 100 samples. The Fig. 4 not only demonstrates that FEDL outperforms

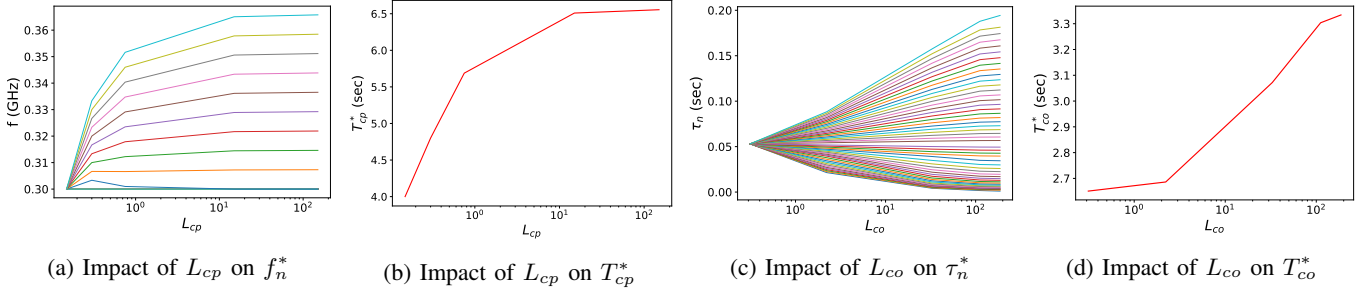


Fig. 6: Impact of UE heterogeneity on SUB1 and SUB2 with  $\kappa = 0.07$ .

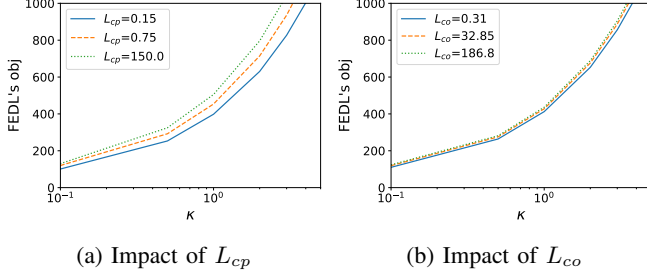


Fig. 7: Impact of UE heterogeneity on FEDL.

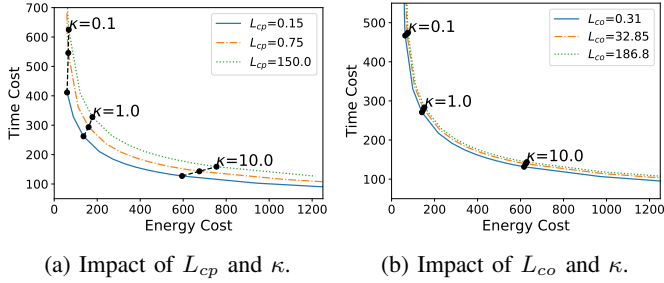


Fig. 8: Pareto-optimal points of FEDL.

FedAvg on all batch size settings (the increase in term of testing accuracy and training loss are approximately 1.7% and 33% respectively for the batchsize 50, 2.1% and 28% for the batchsize 100, and 3.6% and 33% for the full batch size) but also shows that increasing batch size causes the lower convergence speed of both FEDL and FedAvg. Even if using the larger batch size benefits the training time of one local iteration update, it will lead to the grow in value of  $K_l$  to guarantee the FEDL's convergence.

**Effect of increasing local computation on convergence time:** In order to validate the performance of FEDL on a different value of local updates  $K_l$ , in the Fig. 5, we use Mini-Batch SGD algorithm with the fixed batch size of 20 for the local update and increase  $K_l$  from 10 to 50. When  $K_l$  is small, it can be seen that FEDL achieves significant performance gap over FedAvg in terms of training loss and testing accuracy. Although this gap is slightly narrowed with the larger  $K_l$ , the rise of  $K_l$  has an appreciable positive impact on the convergence time of both FEDL and FedAvg. However, it is also remarkable that when  $K_l$  reaches a sufficiently large

value, FEDL will slightly fluctuate.

## VII. NUMERICAL RESULTS

In this section, both the communication and computation models follow the same setting as in Fig. 1, except the number of UEs is increased to 50, and all UEs have the same  $f_n^{max} = 2.0$  GHz and  $c_n = 20$  cycles/bit. Furthermore, we define two new parameters, addressing the UE heterogeneity regarding to computation and communication phases in FEDL, respectively, as follows

$$L_{cp} = \frac{\max_{n \in \mathcal{N}} \frac{c_n D_n}{f_n^{max}}}{\min_{n \in \mathcal{N}} \frac{c_n D_n}{f_n^{min}}} \quad (30)$$

$$L_{co} = \frac{\max_{n \in \mathcal{N}} \tau_n^{min}}{\min_{n \in \mathcal{N}} \tau_n^{max}}. \quad (31)$$

We see that higher values of  $L_{cp}$  and  $L_{co}$  indicate higher levels of UE heterogeneity. For example,  $L_{cp} = 1$  ( $L_{co} = 1$ ) can be considered as high heterogeneity level due to unbalanced data distributed and/or UE configuration (unbalanced channel gain distribution) such that UE with their minimum frequency (maximum transmission power) still have the same computation (communication) time as those with maximum frequency (minimum transmission power). The level of heterogeneity is controlled by two different settings. To vary  $L_{cp}$ , the training size  $D_n$  is generated with the fraction  $\frac{D_n^{min}}{D_n^{max}} \in \{1, 0.2, 0.001\}$  but the average UE data size is kept at the same value 7.5 MB for varying values of  $L_{cp}$ . On the other hand, to vary  $L_{co}$ , the distance between these devices and the edge server is generated such that  $\frac{d_n^{min}}{d_n^{max}} \in \{1, 0.2, 0.001\}$  but the average distance of all UEs is maintained at 26 m for different values of  $L_{co}$ . Here  $D_n^{min}$  and  $D_n^{max}$  ( $d_n^{min}$  and  $d_n^{max}$ ) are minimum and maximum data size (edge server-to-UE distance), respectively. In all scenarios, we fix  $L_{cp} = 0.3$  when varying  $L_{co}$  and fix  $L_{co} = 0.48$  when varying  $L_{cp}$ .

1) *Impact of UE heterogeneity:* We first examine the impact of UE heterogeneity on SUB1 and SUB2 in Fig. 6, which shows that increasing  $L_{cp}$  and  $L_{co}$  enforces the optimal  $f_n^*$  and  $\tau_n^*$  having more diverse values, and thus makes increase the computation and communication time  $T_{cp}^*$  and  $T_{co}^*$ , respectively. As expected, we observe that the high level of UE heterogeneity has negative impact on the FEDL system, as illustrated in Figs. 8a and 8b, such that the total cost (objective of FEDL) is increased with higher value of  $L_{cp}$  and  $L_{co}$

respectively. However, in this setting, when  $T_{cp}$  is comparable to  $T_{co}$ , e.g., 6.2 versus 2.9 seconds at  $L_{cp} = L_{co} = 10$ , the impacts of  $L_{cp}$  and  $L_{co}$  on total cost are comparable, e.g., at  $\kappa = (0.1, 1, 10)$ , the total cost of FEDL increases (1.09, 1.14, 1.13) times and (1.08, 1.04, 1.04) times, when  $L_{cp}$  and  $L_{co}$  are increased from 0.15 to 150, and from 0.31 to 186.8, respectively.

On the other hand, with a different setting such that  $T_{cp}$  dominates  $T_{co}$ , e.g., 80 versus 7.8 seconds at  $L_{cp} = L_{co} = 10$ , the impact of  $L_{co}$  on the total cost is more profound than that of  $L_{cp}$ , e.g., at  $\kappa = (0.1, 1, 10)$ , the total cost of FEDL increases (1.29, 1.27, 1.26) times and (1.13, 1.06, 1.07) times, when  $L_{cp}$  and  $L_{co}$  are increased from 0.05 to 50, and from 0.17 to 181.42, respectively.

2) *Pareto Optimal trade-off*: We next illustrate the Pareto curve in Fig. 8. This curve shows the trade-off between the conflicting goals of minimizing the time cost  $K(\theta)T_g$  and energy cost  $K(\theta)E_g$ , in which we can decrease one type of cost yet with the expense of increasing the other one. This figure also shows that the Pareto curve of FEDL is more efficient when the system has low level of UE heterogeneity (i.e., small  $L_{cp}$  and/or  $L_{co}$ ).

## VIII. CONCLUSIONS AND FUTURE WORKS

In this paper, we studied a decentralized machine learning scheme, FL, in which the training model is distributed to participating UEs performing training computation over their local data. Although FL shows vital advantages in data privacy, the heterogeneity across users data and UEs' characteristics are still challenging problems. In order to tackle the heterogeneous data, we proposed an effective algorithm without the i.i.d. UEs' data assumption for strongly convex and smooth FL's problems and then characterize the convergence trade-off between local and global communication rounds. For the wireless resource allocation problem, we embedded the proposed FL algorithm in wireless networks which considers the trade-offs not only between computation and communication latencies but also the Federated Learning time and UE energy consumption. Despite the non-convex nature of this problem, we decomposed it into three sub-problems with convex structure before analyzing their closed-form solutions and quantitative insights into problem design. We then verified the theoretical findings of the new algorithm by experiments on Tensorflow with several federated datasets, and the wireless resource allocation sub-problems by extensive numerical results. In addition to validating the theoretical convergence, our experiments also showed that the proposed algorithm can boost the convergence speed compared to an existing baseline approach.

## REFERENCES

- [1] N. H. Tran, W. Bao, A. Zomaya, M. N. Nguyen, and C. S. Hong, "Federated Learning over Wireless Networks: Optimization Model Design and Analysis," in *IEEE INFOCOM 2019*, Paris, France, Apr. 2019.
- [2] D. Reinsel, J. Gantz, and J. Rydning, "The Digitization of the World from Edge to Core," p. 28, 2018.
- [3] "Free Community-based GPS, Maps & Traffic Navigation App — Waze," <https://www.waze.com/>.
- [4] W. H. Report, "Consumer Data Privacy in a Networked World: A Framework for Protecting Privacy and Promoting Innovation in the Global Digital Economy," *Journal of Privacy and Confidentiality*, Mar. 2013.
- [5] B. McMahan, E. Moore, D. Ramage, S. Hampson, and B. A. y Arcas, "Communication-Efficient Learning of Deep Networks from Decentralized Data," in *Artificial Intelligence and Statistics*, Apr. 2017, pp. 1273–1282.
- [6] <https://www.techradar.com/news/what-does-ai-in-a-phone-really-mean>.
- [7] J. Konečný, H. B. McMahan, D. Ramage, and P. Richtárik, "Federated Optimization: Distributed Machine Learning for On-Device Intelligence," *arXiv:1610.02527 [cs]*, Oct. 2016.
- [8] S. Wang, T. Tuor, T. Salonidis, K. K. Leung, C. Makaya, T. He, and K. Chan, "Adaptive Federated Learning in Resource Constrained Edge Computing Systems," *IEEE Journal on Selected Areas in Communications*, vol. 37, no. 6, pp. 1205–1221, Jun. 2019.
- [9] V. Smith, S. Forte, C. Ma, M. Takáč, M. I. Jordan, and M. Jaggi, "Co-CoA: A General Framework for Communication-Efficient Distributed Optimization," *Journal of Machine Learning Research*, vol. 18, no. 230, pp. 1–49, 2018.
- [10] A. K. Sahu, T. Li, M. Sanjabi, M. Zaheer, A. Talwalkar, and V. Smith, "Federated Optimization for Heterogeneous Networks," *arXiv:1812.06127 [cs, stat]*, Dec. 2018.
- [11] C. Ma, J. Konečný, M. Jaggi, V. Smith, M. I. Jordan, P. Richtárik, and M. Takáč, "Distributed optimization with arbitrary local solvers," *Optimization Methods and Software*, vol. 32, no. 4, pp. 813–848, Jul. 2017.
- [12] J. Hamm, A. C. Champion, G. Chen, M. Belkin, and D. Xuan, "Crowd-ML: A Privacy-Preserving Learning Framework for a Crowd of Smart Devices," in *IEEE ICDCS*, Jun. 2015, pp. 11–20.
- [13] O. Shamir, N. Srebro, and T. Zhang, "Communication-efficient Distributed Optimization Using an Approximate Newton-type Method," in *ICML*, Beijing, China, 2014, pp. II–1000–II–1008.
- [14] J. Wang and G. Joshi, "Cooperative SGD: A unified Framework for the Design and Analysis of Communication-Efficient SGD Algorithms," *arXiv:1808.07576 [cs, stat]*, Aug. 2018.
- [15] S. U. Stich, "Local SGD Converges Fast and Communicates Little," *arXiv:1805.09767 [cs, math]*, May 2018.
- [16] F. Zhou and G. Cong, "On the convergence properties of a  $\$K\$$ -step averaging stochastic gradient descent algorithm for nonconvex optimization," *arXiv:1708.01012 [cs, stat]*, Aug. 2017.
- [17] J. Konečný, H. B. McMahan, F. X. Yu, P. Richtárik, A. T. Suresh, and D. Bacon, "Federated Learning: Strategies for Improving Communication Efficiency," <http://arxiv.org/abs/1610.05492>, Oct. 2016.
- [18] V. Smith, C.-K. Chiang, M. Sanjabi, and A. Talwalkar, "Federated Multi-task Learning," in *NIPS'17*. USA: Curran Associates Inc., 2017, pp. 4427–4437.
- [19] S. J. Reddi, J. Konečný, P. Richtárik, B. Póczós, and A. Smola, "AIDE: Fast and Communication Efficient Distributed Optimization," *arXiv:1608.06879 [cs, math, stat]*, Aug. 2016.
- [20] M. M. Amiri and D. Gündüz, "Over-the-Air Machine Learning at the Wireless Edge," in *2019 IEEE 20th International Workshop on Signal Processing Advances in Wireless Communications (SPAWC)*, Jul. 2019, pp. 1–5.
- [21] H. Tang, S. Gan, C. Zhang, T. Zhang, and J. Liu, "Communication Compression for Decentralized Training," in *NeurIPS*, 2018, pp. 7663–7673.
- [22] T. T. Vu, D. T. Ngo, N. H. Tran, H. Q. Ngo, M. N. Dao, and R. H. Middleton, "Cell-Free Massive MIMO for Wireless Federated Learning," *arXiv:1909.12567 [cs, eess, math]*, Sep. 2019.
- [23] H. Wang, S. Sievert, S. Liu, Z. Charles, D. Papailiopoulos, and S. Wright, "ATOMO: Communication-efficient Learning via Atomic Sparsification," in *NeurIPS*, 2018, pp. 9850–9861.
- [24] H. Zhang, J. Li, K. Kara, D. Alistarh, J. Liu, and C. Zhang, "ZipML: Training Linear Models with End-to-End Low Precision, and a Little Bit of Deep Learning," in *International Conference on Machine Learning*, Jul. 2017, pp. 4035–4043.
- [25] A. Banerjee, S. Merugu, I. S. Dhillon, and J. Ghosh, "Clustering with Bregman Divergences," *Journal of Machine Learning Research*, vol. 6, pp. 1705–1749, Dec. 2005.
- [26] Y. Nesterov, *Lectures on Convex Optimization*. Springer International Publishing, 2018, vol. 137.

- [27] A. P. Miettinen and J. K. Nurminen, "Energy Efficiency of Mobile Clients in Cloud Computing," in *USENIX HotCloud'10*, Berkeley, CA, USA, 2010, pp. 4–4.
- [28] T. D. Burd and R. W. Brodersen, "Processor Design for Portable Systems," *Journal of VLSI Signal Processing System*, vol. 13, no. 2–3, pp. 203–221, Aug. 1996.
- [29] B. Prabhakar, E. U. Bıyıkoglu, and A. E. Gamal, "Energy-efficient transmission over a wireless link via lazy packet scheduling," in *IEEE INFOCOM 2001*, vol. 1, 2001, pp. 386–394.
- [30] S. Boyd and L. Vandenberghe, *Convex Optimization*. Cambridge University Press, Mar. 2004.
- [31] A. Wächter and L. T. Biegler, "On the implementation of an interior-point filter line-search algorithm for large-scale nonlinear programming," *Mathematical Programming*, vol. 106, no. 1, pp. 25–57, Mar. 2006.
- [32] C. Dinh, [https://github.com/CharlieDinh/FEDL\\_Over\\_WireLess](https://github.com/CharlieDinh/FEDL_Over_WireLess).
- [33] Y. Lecun, L. Bottou, Y. Bengio, and P. Haffner, "Gradient-based learning applied to document recognition," *Proceedings of the IEEE*, vol. 86, no. 11, pp. 2278–2324, Nov./1998.
- [34] S. Caldas, P. Wu, T. Li, J. Konečný, H. B. McMahan, V. Smith, and A. Talwalkar, "LEAF: A Benchmark for Federated Settings," *arXiv:1812.01097 [cs, stat]*, Dec. 2018.
- [35] G. Cohen, S. Afshar, J. Tapson, and A. van Schaik, "EMNIST: Extending MNIST to handwritten letters," in *2017 International Joint Conference on Neural Networks (IJCNN)*, May 2017, pp. 2921–2926.

## APPENDIX

### A. Review of useful existing results

With Assumption 1 on  $L$ -smoothness and  $\beta$ -strong convexity of  $F_n(\cdot)$ , according to [26][Theorems 2.1.5 and 2.1.10], we have the following useful inequalities

$$2L(F_n(w) - F_n(w^*)) \geq \|\nabla F_n(w)\|^2, \forall w. \quad (32)$$

$$\langle \nabla F_n(w) - \nabla F_n(w'), w - w' \rangle \geq \frac{1}{L} \|\nabla F_n(w) - \nabla F_n(w')\|^2, \forall w, w' \quad (33)$$

$$2\beta(F_n(w) - F_n(w^*)) \leq \|\nabla F_n(w)\|^2, \forall w. \quad (34)$$

$$\beta \|w - w^*\| \leq \|\nabla F_n(w)\|, \forall w. \quad (35)$$

where  $w^*$  is the solution to problem  $\min_{w \in \mathbb{R}^d} F_n(w)$ , i.e.,  $\nabla F_n(w^*) = 0$ .

### B. Proof of Lemma 1

Due to  $L$ -smooth and  $\beta$ -strongly convex  $J_n$ , from (32) and (34), respectively, we have

$$\begin{aligned} J_n^t(z_k) - J_n^t(z^*) &\geq \frac{\|\nabla J_n^t(z_k)\|^2}{2L}, \\ J_n^t(z_0) - J_n^t(z^*) &\leq \frac{\|\nabla J_n^t(z_0)\|^2}{2\beta} \end{aligned}$$

Combining these inequalities with (8), and setting  $z_0 = w^{t-1}$  and  $z_k = w_n^t$ , we have

$$\|\nabla J_n^t(w_n^t)\|^2 \leq c \frac{L}{\beta} (1 - \gamma)^k \|\nabla J_n^t(w^{t-1})\|^2$$

Since  $(1 - \gamma)^k \leq e^{-k\gamma}$ , the  $\theta$ -approximation condition (4) is satisfied when

$$c \frac{L}{\beta} e^{-k\gamma} \leq \theta^2.$$

Taking log both sides of the above, we complete the proof.

### C. Proof of Theorem 1

We remind the definition of  $J_n^t(w)$  as follows

$$J_n^t(w) = F_n(w) + \langle \eta \nabla F(w^{t-1}) - \nabla F_n(w^{t-1}), w \rangle. \quad (36)$$

Then, denoting  $\hat{w}_n^t$  the optimal solution to  $\min_{w \in \mathbb{R}^d} J_n^t(w)$ , we have

$$\nabla J_n^t(w^{t-1}) = \eta \nabla F(w^{t-1}), \quad (37)$$

$$\nabla J_n^t(\hat{w}_n^t) = 0 = \nabla F_n(\hat{w}_n^t) + \eta \nabla F(w^{t-1}) - \nabla F_n(w^{t-1}). \quad (38)$$

Since  $F(\cdot)$  is also  $L$ -Lipschitz smooth (i.e.,  $\|\nabla F(w) - \nabla F(w')\| \leq \sum_{n=1}^N \frac{D_n}{D} \|\nabla F_n(w) - \nabla F_n(w')\| \leq L \|w - w'\|, \forall w, w'$ , by using Jensen's inequality and  $L$ -smoothness, respectively), we have

$$\begin{aligned} F(w_n^t) - F(w^{t-1}) &\leq \langle \nabla F(w^{t-1}), w_n^t - w^{t-1} \rangle + \frac{L}{2} \|w_n^t - w^{t-1}\|^2 \\ &\stackrel{(38)}{\leq} -\frac{1}{\eta} \langle \nabla F_n(\hat{w}_n^t) - \nabla F_n(w^{t-1}), w_n^t - w^{t-1} \rangle + \frac{L}{2} \|w_n^t - w^{t-1}\|^2 \\ &= -\frac{1}{\eta} \langle \nabla F_n(\hat{w}_n^t) - \nabla F_n(w_n^t), w_n^t - w^{t-1} \rangle + \frac{L}{2} \|w_n^t - w^{t-1}\|^2 \\ &\quad - \frac{1}{\eta} \langle \nabla F_n(w_n^t) - \nabla F_n(w^{t-1}), w_n^t - w^{t-1} \rangle \end{aligned} \quad (39)$$

$$\begin{aligned} &\leq \frac{L}{\eta} \|\hat{w}_n^t - w_n^t\| \|w_n^t - w^{t-1}\| + \frac{L}{2} \|w_n^t - w^{t-1}\|^2 \\ &\quad - \frac{1}{\eta} \langle \nabla F_n(w_n^t) - \nabla F_n(w^{t-1}), w_n^t - w^{t-1} \rangle \end{aligned} \quad (40)$$

$$\begin{aligned} &\stackrel{(33)}{\leq} \frac{L}{\eta} \|\hat{w}_n^t - w_n^t\| \|w_n^t - w^{t-1}\| + \frac{L}{2} \|w_n^t - w^{t-1}\|^2 \\ &\quad - \frac{1}{\eta L} \|\nabla F_n(w_n^t) - \nabla F_n(w^{t-1})\|^2, \end{aligned} \quad (41)$$

where (39) is by adding and subtracting  $\nabla F_n(w_n^t)$ , and we have (40) by using Cauchy-Schwartz inequality and  $L$ -Lipschitz smoothness of  $F_n(\cdot)$ . Before continuing the convergence proof, we have following useful results

$$\begin{aligned} \|\hat{w}_n^t - w_n^t\| &\stackrel{(35)}{\leq} \frac{1}{\beta} \|\nabla J_n^t(w_n^t)\| \stackrel{(4)}{\leq} \frac{\theta}{\beta} \|\nabla J_n^t(w^{t-1})\| \\ &\stackrel{(37)}{=} \frac{\theta \eta}{\beta} \|\nabla F(w^{t-1})\|, \end{aligned} \quad (42)$$

$$\|\hat{w}_n^t - w^{t-1}\| \stackrel{(35)}{\leq} \frac{1}{\beta} \|\nabla J_n^t(w^{t-1})\| \stackrel{(37)}{=} \frac{\eta}{\beta} \|\nabla F(w^{t-1})\|. \quad (43)$$

Using triangle inequality and (42) and (43), we have

$$\begin{aligned} \|w_n^t - w^{t-1}\| &\leq \|w_n^t - \hat{w}_n^t\| + \|\hat{w}_n^t - w^{t-1}\| \\ &\leq (1 + \theta) \frac{\eta}{\beta} \|\nabla F(w^{t-1})\|. \end{aligned} \quad (44)$$

We also have

$$\begin{aligned} \|\nabla F_n(w_n^t) - \nabla F_n(w^{t-1})\| &\stackrel{(36)}{=} \|\nabla J_n^t(w_n^t) - \nabla J_n^t(w^{t-1})\| \\ &\geq \|\nabla J_n^t(w^{t-1})\| - \|\nabla J_n^t(w_n^t)\| \\ &\stackrel{(4)}{\geq} (1 - \theta) \|\nabla J_n^t(w^{t-1})\| \\ &\stackrel{(37)}{=} (1 - \theta) \eta \|\nabla F(w^{t-1})\|. \end{aligned} \quad (45)$$

By substituting (44) and (45) into (41), we have

$$\begin{aligned} & F(w_n^t) - F(w^{t-1}) \\ & \leq -\frac{\eta L}{\beta^2} \left[ (1-\theta)^2 \frac{\beta^2}{L^2} - \theta(1+\theta) - (1+\theta)^2 \frac{\eta}{2} \right] \|\nabla F(w^{t-1})\|^2 \\ & \stackrel{(34)}{\leq} -\frac{2\eta L}{\beta} \left[ (1-\theta)^2 \frac{\beta^2}{L^2} - \theta(1+\theta) - (1+\theta)^2 \frac{\eta}{2} \right] (F(w^{t-1}) - F(w^*)) \end{aligned} \quad (46)$$

$$\stackrel{(11)}{=} -\Theta (F(w^{t-1}) - F(w^*)), \quad (47)$$

where (46) is due to the convexity of  $F_n(\cdot)$ , thus  $F(\cdot)$ . By subtracting  $F(w^*)$  from both sides of (47), we have

$$F(w_n^t) - F(w^*) \leq (1-\Theta) (F(w^{t-1}) - F(w^*)). \quad (48)$$

Finally we have

$$F(w^t) - F(w^*) \leq \sum_{n=1}^N \frac{D_n}{D} (F(w_n^t) - F(w^*)) \quad (49)$$

$$\stackrel{(48)}{\leq} (1-\Theta) (F(w^{t-1}) - F(w^*)), \quad (50)$$

where (49) is due to the convexity of  $F(\cdot)$ .

#### D. Proof of Lemma 2

The convexity of SUB1 can be shown by its strictly convex objective in (13) and its constraints determine a convex set. Thus, the global optimal solution of SUB1 can be found using KKT condition [30]. In the following, we first provide the KKT condition of SUB1, then show that solution in Lemma 2 satisfy this condition.

The Lagrangian of SUB1 is

$$\begin{aligned} L = \sum_{n=1}^N & \left[ E_{n,cp} + \lambda_n \left( \frac{c_n D_n}{f_n} - T_{cp} \right) \right. \\ & \left. + \mu_n (f_n - f_n^{max}) - \nu_n (f_n - f_n^{min}) \right] + \kappa \log(1/\theta) T_{cp} \end{aligned}$$

where  $\lambda_n, \mu_n, \nu_n$  are non-negative dual variables with their optimal values denoted by  $\lambda_n^*, \mu_n^*, \nu_n^*$ , respectively. Then the KKT condition is as follows:

$$\frac{\partial L}{\partial f_n} = \frac{\partial E_{n,cp}}{\partial \tau_n} - \lambda_n \frac{c_n D_n}{f_n^2} + \mu_n - \nu_n = 0, \quad \forall n \quad (51)$$

$$\frac{\partial L}{\partial T_{cp}} = \kappa - \sum_{n=1}^N \lambda_n = 0, \quad (52)$$

$$\mu_n (f_n - f_n^{max}) = 0, \quad \forall n \quad (53)$$

$$\nu_n (f_n - f_n^{min}) = 0, \quad \forall n \quad (54)$$

$$\lambda_n \left( \frac{c_n D_n}{f_n} - T_{cp} \right) = 0, \quad \forall n \quad (55)$$

Next, we will show that the optimal solution according to KKT condition is also the same as that provided by Lemma 2. To do that, we observe that the existence of  $\mathcal{N}_1, \mathcal{N}_2, \mathcal{N}_3$  and their respective  $T_{\mathcal{N}_1}, T_{\mathcal{N}_2}, T_{\mathcal{N}_3}$  produced by Algorithm 2 depends on  $\kappa$ . Therefore, we will construct the ranges of  $\kappa$  such that there exist three subsets  $\mathcal{N}'_1, \mathcal{N}'_2, \mathcal{N}'_3$  of UEs satisfying KKT condition and having the same solution as that in Lemma 2 in the following cases.

a)  $T_{cp}^* = T_{\mathcal{N}_1} \geq \max\{T_{\mathcal{N}_2}, T_{\mathcal{N}_3}\}$ : This happens when  $\kappa$  is large enough so that the condition in line 4 of Algorithm 2 satisfies because  $T_{\mathcal{N}_3}$  is decreasing when  $\kappa$  increase. Thus we consider  $\kappa \geq \sum_{n=1}^N \alpha_n (f_n^{max})^3$  (which ensures  $\mathcal{N}_1$  of Algorithm 2 is non-empty).

From (52), we have

$$\kappa = \sum_{n=1}^N \lambda_n^*, \quad (56)$$

thus  $\kappa$  in this range can guarantee a non-empty set  $\mathcal{N}'_1 = \{n | \lambda_n^* \geq \alpha_n (f_n^{max})^3\}$  such that

$$\frac{\partial E_{n,cp}(f_n^*)}{\partial f_n} - \lambda_n^* \frac{c_n D_n}{f_n^{*2}} \leq 0, \quad \forall n \in \mathcal{N}'_1 : f_n^* \leq f_n^{max}.$$

Then from (51) we must have  $\mu_n^* - \nu_n^* \geq 0$ , thus, according to (53)  $f_n^* = f_n^{max}, \forall n \in \mathcal{N}'_1$ . From (55), we see that  $\mathcal{N}'_1 = \{n : \frac{c_n D_n}{f_n^{max}} = T_{cp}^*\}$ . Hence, by the definition in (19),

$$T_{cp}^* = \max_{n \in \mathcal{N}} \frac{c_n D_n}{f_n^{max}}. \quad (57)$$

On the other hand, if there exist a non-empty set  $\mathcal{N}'_2 = \{n | \lambda_n^* = 0\}$ , it must be due to

$$\frac{c_n D_n}{f_n^{min}} \leq T_{cp}^*, \quad \forall n \in \mathcal{N}'_2$$

according to (55). In this case, from (51) we must have  $\mu_n^* - \nu_n^* \leq 0 \Rightarrow f_n^* = f_n^{min}, \forall n \in \mathcal{N}'_2$ .

Finally, if there exists UEs with  $\frac{c_n D_n}{f_n^{min}} > T_{cp}^*$  and  $\frac{c_n D_n}{f_n^{max}} < T_{cp}^*$ , they will belong to the set  $\mathcal{N}'_3 = \{n | \alpha_n (f_n^{min})^3 < \lambda_n^* < \alpha_n (f_n^{max})^3\}$  such that  $f_n^{min} < f_n^* < f_n^{max}$ . According to (55),  $T_{cp}^*$  must be the same for all  $n$  with  $\lambda_n^* > 0$ , we obtain

$$f_n^* = \frac{c_n D_n}{T_{cp}^*} = \frac{c_n D_n}{\max_n \frac{c_n D_n}{f_n^{max}}}, \quad \forall n \in \mathcal{N}'_3. \quad (58)$$

In summary, we have

$$f_n^* = \begin{cases} f_n^{max}, & \forall n \in \mathcal{N}'_1 \\ f_n^{min}, & \forall n \in \mathcal{N}'_2 \\ \frac{c_n D_n}{T_{cp}^*}, & \forall n \in \mathcal{N}'_3 \end{cases}$$

with  $T_{cp}^*$  determined in (57).

b)  $T_{cp}^* = T_{\mathcal{N}_2} > \max\{T_{\mathcal{N}_1}, T_{\mathcal{N}_3}\}$ : This happens when  $\kappa$  is small enough such that the condition in line 7 of Algorithm 2 satisfies. In this case,  $\mathcal{N}_1$  is empty and  $\mathcal{N}_2$  is non-empty according to line 8 of this algorithm. Thus we consider  $\kappa \leq \sum_{n=1}^N \alpha_n (f_n^{min})^3$ . Due to the considered small  $\kappa$  and (56), there must exist a non-empty set  $\mathcal{N}'_2 = \{n : \lambda_n^* \leq \alpha_n (f_n^{min})^3\}$  such that

$$\frac{\partial E_{n,cp}(f_n^*)}{\partial f_n} - \lambda_n^* \frac{c_n D_n}{f_n^{*2}} \geq 0, \quad \forall n \in \mathcal{N}'_2 : f_n^* \geq f_n^{min}.$$

Then, from (51) we must have  $\mu_n^* - \nu_n^* \leq 0$ , and thus from (53),  $f_n^* = f_n^{min}, \forall n \in \mathcal{N}'_2$ . Therefore, by the definition (19) we have

$$T_{cp}^* = \max_{n \in \mathcal{N}'_2} \frac{c_n D_n}{f_n^{min}}.$$

If we further restrict  $\kappa \leq \min_{n \in \mathcal{N}} \alpha_n (f_n^{min})^3$ , then we see that  $\mathcal{N}'_2 = \mathcal{N}$ , i.e.,  $f_n^* = f_n^{min}, \forall n \in \mathcal{N}$ . On the other hand, if we consider  $\sum_{n=1}^N \alpha_n (f_n^{min})^3 < \kappa \leq \min_{n \in \mathcal{N}} \alpha_n (f_n^{min})^3$ , then there may exist UEs with  $\frac{c_n D_n}{f_n^{min}} > T_{cp}^*$  and  $\frac{c_n D_n}{f_n^{max}} < T_{cp}^*$ , which will belong to the set  $\mathcal{N}'_3 = \{n | \alpha_n (f_n^{min})^3 < \lambda_n^* < \alpha_n (f_n^{max})^3\}$  such that

$f_n^{min} < f_n^* < f_n^{max}, \forall n \in \mathcal{N}'_3$ . Then, according to (55),  $T_{cp}^*$  must be the same for all  $n$  with  $\lambda_n^* > 0$ , we obtain

$$f_n^* = \frac{c_n D_n}{T_{cp}^*} = \frac{c_n D_n}{\max_n \frac{c_n D_n}{f_n^{min}}}, \quad \forall n \in \mathcal{N}'_3. \quad (59)$$

In summary, we have

$$f_n^* = \begin{cases} \frac{c_n D_n}{T_{cp}^*}, & \forall n \in \mathcal{N}'_3 \\ f_n^{min}, & \forall n \in \mathcal{N}'_2 \end{cases}$$

- c)  $T_{cp}^* = T_{N_3} > \max\{T_{N_1}, T_{N_2}\}$ : This happens when  $\kappa$  is between a range such that in Algorithm 2, the condition at line 7 is violated at some round, while the condition at line 4 not satisfied. In this case,  $\mathcal{N}_1$  is empty and  $\mathcal{N}_3$  is non-empty according to line 8 of this algorithm. Thus we consider  $\sum_{n=1}^N \alpha_n (f_n^{min})^3 < \kappa < \sum_{n=1}^N \alpha_n (f_n^{max})^3$ . With this range of  $\kappa$ , and (56), there must exist a non-empty set  $\mathcal{N}'_3 = \{n | \alpha_n (f_n^{min})^3 < \lambda_n^* < \alpha_n (f_n^{max})^3\}$  such that  $f_n^{min} < f_n^* < f_n^{max}, \forall n \in \mathcal{N}'_3$ . Then, from (51) we have  $\mu_n^* - \nu_n^* = 0$  and the following equation

$$\frac{\partial E_{n,cp}(f_n)}{\partial f_n} - \lambda_n^* \frac{c_n D_n}{f_n^2} = 0$$

has its solution  $f_n^* = \left(\frac{\lambda_n^*}{\alpha_n}\right)^{1/3}, \forall n \in \mathcal{N}'_3$ . Furthermore, from (55), we have

$$\frac{c_n D_n}{f_n^*} = c_n D_n \left(\frac{\alpha_n}{\lambda_n^*}\right)^{1/3} = T_{cp}^*, \quad \forall n \in \mathcal{N}'_3. \quad (60)$$

Combining (60) with (56), we have

$$T_{cp}^* = \left(\frac{\sum_{n \in \mathcal{N}'_3} \alpha_n (c_n D_n)^3}{\kappa}\right)^{1/3}.$$

On the other hand, if there exist a non-empty set  $\mathcal{N}'_2 = \{n | \lambda_n^* = 0\}$ , it must be due to

$$\frac{c_n D_n}{f_n^{min}} < T_{cp}^*, \quad \forall n \in \mathcal{N}'_2$$

according to (55). From (51) we must have  $\mu_n^* - \nu_n^* \leq 0 \Rightarrow f_n^* = f_n^{min}, \forall n \in \mathcal{N}'_2$ . In summary, we have

$$f_n^* = \begin{cases} \frac{c_n D_n}{T_{cp}^*}, & \forall n \in \mathcal{N}'_3 \\ f_n^{min}, & \forall n \in \mathcal{N}'_2 \end{cases}$$

Considering all cases above, we see that the solutions characterized by KKT condition above are exactly the same as those provided in Lemma 2.

### E. Proof of Lemma 3

According to (16) and (17), the objective of SUB2 is the sum of perspective functions of convex and linear functions, and its constraints determine a convex set; thus SUB2 is a convex problem that can be analyzed using KKT condition [30].

The Lagrangian of SUB2 is

$$L = \sum_{n=1}^N E_{n,co}(\tau_n) + \lambda(\sum_{n=1}^N \tau_n - T_{co}) + \sum_{n=1}^N \mu_n(\tau_n - \tau_n^{max}) - \sum_{n=1}^N \nu_n(\tau_n - \tau_n^{min}) + \kappa T_{co}$$

where  $\lambda, \mu_n, \nu_n$  are non-negative dual variables. Then the KKT condition is as follows:

$$\frac{\partial L}{\partial \tau_n} = \frac{\partial E_{n,co}}{\partial \tau_n} + \lambda + \mu_n - \nu_n = 0, \quad \forall n \quad (61)$$

$$\frac{\partial L}{\partial T_{co}} = \kappa - \lambda = 0, \quad (62)$$

$$\mu_n(\tau_n - \tau_n^{max}) = 0, \quad \forall n \quad (63)$$

$$\nu_n(\tau_n - \tau_n^{min}) = 0, \quad \forall n \quad (64)$$

$$\lambda(\sum_{n=1}^N \tau_n - T_{co}) = 0. \quad (65)$$

From (62), we see that  $\lambda^* = \kappa$ . Let  $x := \frac{s_n}{\tau_n B}$ , we first consider the equation

$$\begin{aligned} \frac{\partial E_{n,co}}{\partial \tau_n} + \lambda^* &= 0 \Leftrightarrow \frac{N_0}{h_n}(e^x - 1 - xe^x) = -\lambda^* = -\kappa \\ \Leftrightarrow e^x(x-1) &= \kappa N_0^{-1} h_n - 1 \\ \Leftrightarrow e^{x-1}(x-1) &= \frac{\kappa N_0^{-1} h_n - 1}{e} \\ \Leftrightarrow x &= 1 + W\left(\frac{\kappa N_0^{-1} h_n - 1}{e}\right) \\ \Leftrightarrow \tau_n &= g_n(\kappa) = \frac{s_n/B}{1 + W\left(\frac{\kappa N_0^{-1} h_n - 1}{e}\right)}. \end{aligned}$$

Because  $W(\cdot)$  is strictly increasing when  $W(\cdot) > -\ln 2$ ,  $g_n(\kappa)$  is strictly decreasing and positive, and so is its inverse function

$$g_n^{-1}(\tau_n) = -\frac{\partial E_{n,co}(\tau_n)}{\partial \tau_n}.$$

Then we have

- a) If  $g_n(\kappa) \leq \tau_n^{min} \Leftrightarrow \kappa \geq g_n^{-1}(\tau_n^{min})$ , then we have

$$\kappa = \lambda^* \geq g_n^{-1}(\tau_n^{min}) \geq -\frac{\partial E_{n,co}}{\partial \tau_n} \Big|_{\tau_n^{min} \leq \tau_n}.$$

Thus, according to (61),  $\mu_n^* - \nu_n^* \leq 0$ . Because both  $\mu_n^*$  and  $\nu_n^*$  cannot be positive, we have  $\mu_n^* = 0$  and  $\nu_n^* \geq 0$ . Then we consider two cases of  $\nu^*$ : a)  $\nu_n^* > 0$ , from (64),  $\tau_n^* = \tau_n^{min}$ , and b)  $\nu_n^* = 0$ , from (61), we must have  $\kappa = g_n^{-1}(\tau_n^{min})$ , and thus  $\tau_n^* = \tau_n^{min}$ .

- b) If  $g_n(\kappa) \geq \tau_n^{max} \Leftrightarrow \kappa \leq g_n^{-1}(\tau_n^{max})$ , then we have

$$\kappa = \lambda^* \leq g_n^{-1}(\tau_n^{max}) \leq -\frac{\partial E_{n,co}}{\partial \tau_n} \Big|_{\tau_n \leq \tau_n^{max}}.$$

Thus, according to (61),  $\mu_n^* - \nu_n^* \geq 0$ , inducing  $\nu_n^* = 0$  and  $\mu_n^* \geq 0$ . With similar reasoning as above, we have  $\tau_n^* = \tau_n^{max}$ .

- c) If  $\tau_n^{min} < g_n(\kappa) < \tau_n^{max} \Leftrightarrow g_n^{-1}(\tau_n^{max}) < \kappa < g_n^{-1}(\tau_n^{min})$ , then from (63) and (64), we must have  $\mu_n^* = \nu_n^* = 0$ , with which and (61) we have

$$\tau_n^* = g_n(\kappa).$$

Finally, with  $\lambda^* = \kappa > 0$ , from (65) we have  $T_{co}^* = \sum_{n=1}^N \tau_n^*$ .